Inorg. Chem. **2003**, *42*, 6667–6672

New Metal-Rich Sulfides Ni_6SnS_2 and $Ni_9Sn_2S_2$ with a 2D Metal Framework: Synthesis, Crystal Structure, and Bonding

A. I. Baranov,[†] A. A. Isaeva,[†] L. Kloo,[‡] and B. A. Popovkin*[,§]

Department of Materials Science, Moscow State University, Leninskie Gory, Moscow, 119992 Russia, Inorganic Chemistry, Royal Institute of Technology, Stockholm, S 100 44 Sweden, and Department of Chemistry, Moscow State University, Leninskie Gory, Moscow, 119992 Russia

Received April 1, 2003

Two new, metal-rich nickel–tin sulfides Ni_6SnS_2 and $Ni_9Sn_2S_2$ were found by establishing phase relations in the ternary Ni–Sn–S system at 540 °C. Their single crystals were prepared by means of chemical vapor transport reactions. Single crystal X-ray diffraction was used for the determination of their crystal structures. Both compounds crystallize in a tetragonal system (*I*4/*mmm*, No. 139, $Z = 2$, $a = 3.646(1)$ Å, $c = 18.151(8)$ Å for Ni_6SnS_2, and $a = 3.678(1)$ Å, $c = 25.527(8)$ Å for $Ni_9Sn_2S_2$). Their crystal structures represent a new structure type and can be considered as assembled from bimetallic nickel–tin and nickel–sulfide slabs alternating along the crystallographic *c* axis. DFT band structure calculations showed the bonding within the bimetallic slabs to have a delocalized, multicenter nature, typical for metallic systems, and predominantly classical, pairwise bonding between nickel and sulfur.

Introduction

Infinite systems of bonds between metal atoms remain intriguing objects for many researchers demonstrating a rich and surprising structural chemistry and interesting physical properties. Striking illustrations are the mixed metal-rich chalcogenides of early transition metals, which form a wide diversity of heterometallic frameworks[1−4] ranging from 1D chains in M_4ETe_4 (M = Nb, Ta; E = Si, Cr, Fe, Co, Ni)[2−4] to 3D frameworks in $Ta_9M_2S_6$ (M = Fe, Co, Ni).[5] Mixed transition−rare earth, metal-rich chalcogenides also have a rich structural chemistry[6] {1D chains in $Sc_{14}M_3Te_8$ (M = Ru, Os),[7] 2D slabs in Sc_6MTe_2 (M = Cu, Ag, Cd),[8] 3D frameworks in $Er_7Ni_2Te_2$[3]}. At the same time, mixed metal-rich chalcogenides of main group and transition metals are much less studied. The best represented family is possibly the mixed antimony−transition metal chalcogenides[9−11] although in most such compounds known so far the Sb atoms play the role of a pnictide ligand rather than a metal atom, for example, sharing position with Se in $Ti_5Sb_{2.2}Se_{0.8}$.[12] The recently synthesized $Ni_{7-x}SbQ_2$ (Q = Se, Te)[10] species have interesting crystal structures which contain unusual bimetallic slabs formed by antimony and Ni atoms. Other p-block metals are known to form a family of compounds with the general composition $T_3M_2Q_2$ (T = Co, Ni, Rh, Pd; M = In, Tl, Sn, Pb, Bi; Q = S, Se) belonging to the parkerite[13] (M = Bi) or shandite[14] structure types both containing 3D bimetallic frameworks.

The systematic study of main group−late transition metal-rich, mixed chalcogenides has recently resulted in the discovery of several new and unusual structures. One example is Ni_8Bi_8SI containing 1D infinite columns formed by Ni and Bi,[15] and $Ni_{151.5}Pb_{24}S_{92}$[16] having a 3D framework

* To whom correspondence should be addressed. E-mail: popovkin@inorg.chem.msu.ru.
† Department of Materials Science, Moscow State University.
‡ Royal Institute of Technology.
§ Department of Chemistry, Moscow State University.

(1) Hughbanks, T. *J. Alloys Compd.* **1995**, *229*, 40.
(2) Badding, M. E.; DiSalvo, F. J. *Inorg. Chem.* **1990**, *29*, 20, 3952.
(3) Meng, F.; Hughbanks, T. *Inorg. Chem.* **2001**, *40*, 11, 2482.
(4) Neuhausen, J.; Finckh, E. W.; Tremel, W. *Chem. Ber.* **1995**, *128*, 6, 569.
(5) Harbrecht, B.; Franzen, H. F. *J. Less-Common Met.* **1985**, *113*, 349.
(6) Mitchell, K.; Ibers, J. A. *Chem. Rev.* **2002**, *102*, 1929.
(7) Chen, L.; Corbett. J. D. *J. Am. Chem. Soc.* **2003**, *125*, 1170.
(8) Chen, L.; Corbett, J. D. *Inorg. Chem.* **2002**, *41*, 2146.
(9) Lee, C.-S.; Kleinke, H. *Eur. J. Inorg. Chem.* **2002**, 591.
(10) Reynolds, T. K.; Bales, J. G.; DiSalvo, F. J. *Chem. Mater.* **2002**, *14*, 4746.
(11) Lee, C.-S.; Safa-Sefat, A.; Greedan, J. E.; Kleinke, H. *Chem. Mater.* **2003**, *15*, 3, 780.
(12) Kleinke, H. *J. Alloys Compd.* **2002**, *336*, 132.
(13) Clauss, A. *Naturwissenschaften* **1977**. 64.
(14) Range, K.-J.; Rau, F.; Zabel, M.; Paulus, H. *Z. Kristallogr.* **1997**, *212*, 50.
(15) Baranov, A. I.; Kloo, L.; Olenev, A. V.; Popovkin, B. A.; Romanenko, A. I.; Shevelkov, A. V. *J. Am. Chem. Soc.* **2001**, *123*, 12375.

10.1021/ic034349+ CCC: $25.00
Published on Web 09/19/2003

of Ni polyhedra linked by Pb atoms. Recently, we have communicated the synthesis of new mixed nickel−tin chalcogenides with the compositions close to 11:2:4.[17] A detailed systematic search for mixed, metal-rich nickel−tin sulfides undertaken in the present study revealed the existence of two new compounds, Ni_6SnS_2 and $Ni_9Sn_2S_2$. This work also reports their crystal and electronic structures and bonding.

Experimental Section

Study of Phase Relations. The 30 samples having compositions within the metal-rich part of the Ni−Sn−S ternary system were studied. The appropriate mixtures of the elements (all of 99.99% purity powders,[18] 1 g total) were loaded into silica ampules, evacuated (10^{-2} mm Hg), and sealed off. The total annealing time (540 °C, with several intermediate grindings in an agate mortar and reannealings of products pressed into pellets) was 14 days. The phase composition of the samples was studied by X-ray powder diffraction [Cu Kα1, STADI/P diffractometer (Stoe)]. The maximum number of phases found in each sample was equal to 3, thus confirming that equilibrium had been reached.

Synthesis. The stoichoimetric mixtures (Ni/Sn/S = 6:1:2 and 9:2:2) of the elements were annealed in the evacuated silica ampules at 540 °C for 8 days. The products were then ground in an agate mortar, pressed into pellets, and further reannealed under the same conditions several times (2 for Ni_6SnS_2 and 6 for $Ni_9Sn_2S_2$). The grayish powders obtained were identified by powder X-ray diffraction [Cu Kα1, STADI/P diffractometer (Stoe)], which showed good agreement with the theoretical patterns of Ni_6SnS_2 and $Ni_9Sn_2S_2$ generated from the single crystal X-ray diffraction data (see below).

Single crystals were prepared from the vapor phase by means of the chemical transport reaction with I_2 (~0.004 mol/L) in the silica ampules (10 × 100 mm) placed in a horizontal, two-temperature furnace with the temperature range 600 (charge end) to 570 °C (empty end). A 0.1 g portion of annealed sample of the composition Ni/Sn/S = 35:3:12 containing Ni_6SnS_2, $Ni_9Sn_2S_2$, and a small amount of Ni was used as charge. After heating for 2 weeks, the formation of square and octagonal plate silvery crystals (0.1 × 0.1 × 0.01 mm^3) was observed in the cold part of the ampule.

Single-Crystal Diffraction. The crystals were mounted on glass fibers for data collection on a KappaCCD (Bruker-Nonius) diffractometer using Ag Kα radiation. The unit cell determination procedure showed that the crystals of two different compounds had been grown. The data collection and structure refinement parameters are listed in Table 1. Direct methods (SHELXS-97[19]) revealed the positions of Sn and Ni atoms that surround tin. Other sites were then localized by repeated least-squares cycles and $\Delta\rho(x, y, z)$ syntheses with the use of the SHELXL-97 software.[20] One of those sites was found to be occupied by sulfur, while two others are partially occupied by Ni atoms [Ni(3) and Ni(4) in Ni_6SnS_2, and Ni(4) and Ni(5) in $Ni_9Sn_2S_2$] (Table 2). Sulfur atoms do not fit into these sites, since meaningless coordination would result. Semiempirical (for Ni_6SnS_2, SCALEPACK software[21]) and numerical (for $Ni_9Sn_2S_2$, upon explicit crystal shape) absorption corrections were applied. At the final stage, the anisotropic thermal parameters were used for all atoms, and the occupancies of Ni(3), Ni(4) [for Ni_6SnS_2] and Ni(4), Ni(5) [for $Ni_9Sn_2S_2$] sites were also allowed to vary independently for each structure. The refined compositions of the phases were found to be Ni_6SnS_2 and $Ni_{8.93(1)}Sn_2S_2$. For the latter, we suggest the formula $Ni_9Sn_2S_2$ because the refined composition is very close to it and EDX analysis and direct synthesis experiment (see foolowing paragraphs) verified that composition. The refined positional parameters for both crystal structures are listed in Table 2.

Table 1. Crystallographic Data for Ni_6SnS_2 and $Ni_9Sn_2S_2$

formula	Ni_6SnS_2	$Ni_{8.93(1)}Sn_2S_2$
fw	535.07	826.07
space group, Z	$I4/mmm$ (No. 139), 2	$I4/mmm$ (No. 139), 2
lattice params (Å, $Å^3$)	$a = 3.6500(5)$	$a = 3.6710(5)$
	$c = 18.141(2)$	$c = 25.474(2)$
	$V = 241.68(6)$	$V = 343.29(7)$
D_{calcd} (g cm^{-3})	7.353	7.992
λ, Å	0.56090	0.56090
μ, mm^{-1}	149.32	164.64
T, °C	25	−100
R^a (F_o^2), $R_w^{a,b}$ (F_o^2)	0.0486, 0.1094	0.0229, 0.0456

[a] For $F_o^2 > 2\sigma(F_o^2)$. [b] For Ni_6SnS_2: $w^{-1} = \sigma^2(F_o^2) + (0.0517P)^2$ where $P = (F_o^2 + 2F_c^2)/3$. For $Ni_9Sn_2S_2$: $w^{-1} = \sigma^2(F_o^2) + (0.0123P)^2$ where $P = (F_o^2 + 2F_c^2)/3$.

Table 2. Atomic Positions for Ni_6SnS_2 (25 °C) and $Ni_9Sn_2S_2$ (−100 °C)

atom	Wyckoff	x/a	y/b	z/c	SOF	U^{eq}
			Ni_6SnS_2			
Sn	2(a)	0	0	0	1	0.0076(1)
S	4(e)	0	0	0.6793(1)	1	0.0127(4)
Ni(1)	8(g)	0	0.5	0.10598(5)	1	0.0091(1)
Ni(2)	2(b)	0	0	0.5	1	0.0074(2)
Ni(3)	4(e)	0	0	0.2075(2)	0.286(6)	0.021(1)
Ni(4)	4(d)	0	0.5	0.25	0.204(7)	0.014(1)
			$Ni_9Sn_2S_2$			
Sn	4(e)	0	0	0.07446(1)	1	0.0022(1)
S	4(e)	0	0	0.69991(5)	1	0.0059(2)
Ni(1)	4(c)	0	0.5	0	1	0.0022(1)
Ni(2)	8(g)	0	0.5	0.14857(1)	1	0.0033(1)
Ni(3)	4(e)	0	0	0.57227(2)	1	0.0026(1)
Ni(4)	4(e)	0	0	0.7802(1)	0.262(3)	0.0104(8)
Ni(5)	4(d)	0	0.5	0.25	0.205(4)	0.0033(9)

As the single crystal X-ray experiments were carried out at different temperatures for Ni_6SnS_2 and $Ni_9Sn_2S_2$, powder diffraction (Guinier camera FR-552 (Enraf-Nonius), Cu Kα1) was used to evaluate the unit cell parameters for both compounds at ambient temperature. They are $a = 3.646(1)$ Å and $c = 18.151(8)$ Å for Ni_6SnS_2, and $a = 3.678(1)$ Å and $c = 25.527(8)$ Å for $Ni_9Sn_2S_2$.

The phase compositions Ni_6SnS_2 and $Ni_9Sn_2S_2$ were confirmed by direct synthesis of pure phases starting from the elements (see preceding details) and EDX analysis.[22]

Band Structure Calculations. Hybrid DFT calculations (B3LYP exchange correlation potential) were performed using CRYSTAL98[23] program package. Hay−Wadt effective core potentials and basis sets,[24] modified in accordance with the recommendations of the CRYSTAL98 manual[23] for use in calculations of extended systems, were used. The convergence criterion for the SCF energy

(16) Baranov, A. I.; Isaeva, A. A.; Popovkin, B. A.; Shpanchenko, R. V. *Izv. Akad. Nauk, Ser. Khim.* **2002**, *12*, 1983.
(17) Lyubimtsev, A. L.; Isaeva, A. A.; Baranov, A. I.; Fischer, A.; Popovkin, B. A. *Book of Abstracts*; International Workshop: High-Temperature Superconductors and Novel Inorganic Materials Engineering MSU HTSC-VI, Moscow-St. Petersburg, 2001; PIII-10.
(18) Ni powder as received was heated (500 °C) for 3 h in H_2 stream.
(19) Sheldrick, G. M. *SHELXS-97, Program for crystal structure solution*; University of Göttingen: Göttingen, Germany, 1997.
(20) Sheldrick, G. M. *SHELXL-97, Program for crystal structure refinement*; University of Göttingen: Göttingen, Germany, 1997.
(21) (a) *SCALEPACK*; KappaCCD Software, Nonius BV: Delft, The Netherlands, 1998. (b) Otwinowski, Z.; Minor, W. In *Methods in Enzymology*; Carter, C. W., Jr., Sweet, R. M., Eds.; Academic Press: New York, 1997; Vol. 276.

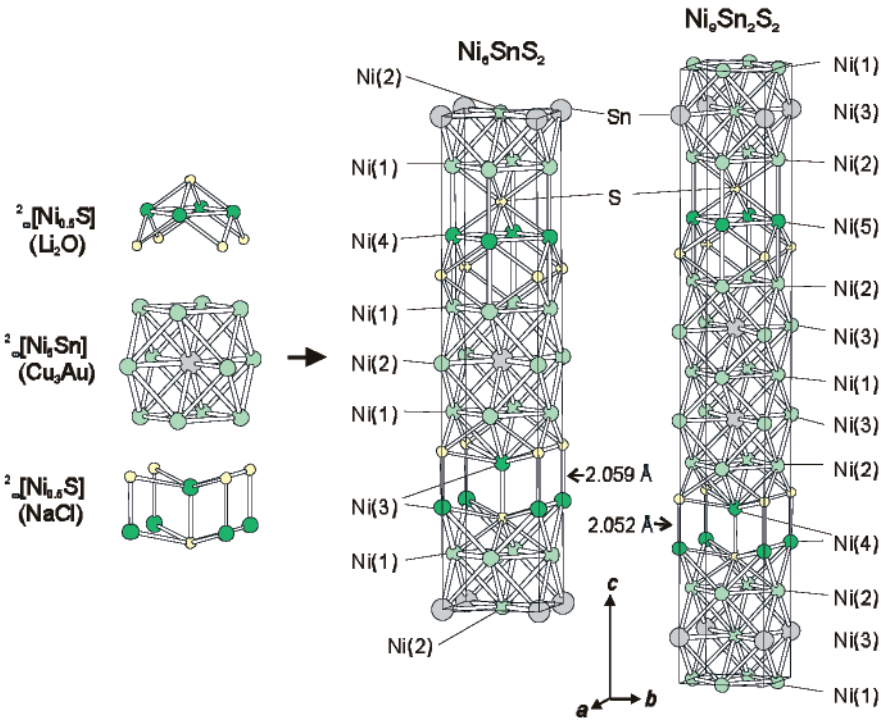

Figure 1. Hypothetical unit cell of the crystal structures of Ni_6SnS_2 and $Ni_9Sn_2S_2$ containing two types of nickel−sulfide slabs. The occupancy of the dark Ni sites is close to $^1/_2$.

was set to 10^{-7} Hartree. The basis set and atomic coordinate sections of CRYSTAL98 input files are available in Supporting Information. Difference charge density plots obtained with the use of TOPOND98[25] and gOpenMol[26] software were analyzed to reveal the main features of the chemical bonding as it was described in refs 15 and 27.

Results

Phase Relation Study. A complete set of the phase relations was established for the metal-rich part (an area enveloped by Ni−Sn−SnS−Ni_7S_6−Ni sections) of the Ni−Sn−S ternary system at 540 °C.[28] Two new compounds, Ni_6SnS_2 and $Ni_9Sn_2S_2$, were found in addition to the already known $Ni_3Sn_2S_2$.[14]

Structure Description. The structure of Ni_6SnS_2 is made from 2D infinite, heterometallic nickel−tin and nickel−sulfide slabs alternating along the *c* axis (Figure 1). Ni−Sn slabs are formed by Sn, Ni(1), and Ni(2) atoms arranged in a Cu_3Au motif. These slabs have the formal composition $^2_\infty[Ni_5Sn]$. The Ni(3) and Ni(4) sites in the sulfide slabs have the occupancy factors close to $^1/_4$, but the calculated shortest distances between different Ni sites within those slabs [*d*(Ni(3)−Ni(4)] are nonphysically short (less than 2.0 Å). In order to avoid such a structural description, it is appropriate to suggest that different types of Ni atoms always reside in different nickel−sulfide slabs, thus being spatially separated. Thus, this suggestion implies a model where two types of nickel−sulfide slabs exist in both structures, each formed by S and only one of two different Ni positions; S and Ni(3) or S and Ni(4). The Ni and S atoms are arranged in distorted NaCl [Ni(3), S] and Li_2O (antifluorite) motifs [Ni(4), S; Figure 1], respectively. It is worth noting that Ni(3) and Ni(4) sites cannot reside in the same Ni−S slab because this would result either in short Ni−Ni contacts or meaningless coordination of S atoms by nickel so that the suggested model looks like the only possible model.

Both types of coordination of Ni by S are common and can be found for example in Ni_9S_8.[29] The S sites in the NaCl and Li_2O slabs have different coordination but merge into one crystallographic position, since thermal motion makes them indistinguishable. Almost equal amounts of rock salt and antifluorite nickel−sulfide slabs are disposed statistically in the structure. The Ni atoms within each Ni−S slab occupy approximately every second position. Therefore, two types of disorder exist in the structure: (1) in the disposition of different Ni−S slabs along the *c* axis and (2) in the disposition of Ni sites inside the slabs.

(22) An analysis of a Ni_6SnS_2 crystal which was used for X-ray diffraction gave the composition (at. %) Ni 68, Sn 10.9, S 21.1 (CAMEBAX microprobe device, accelerating voltage 19kV, the collection time 70 s) which is in agreement with one that resulted from the X-ray experiment (at. %: Ni 66.67, Sn 11.1, S 22.2). An analysis of a $Ni_9Sn_2S_2$ pressed pellet gave the composition (at. %) Ni 69, Sn 15.8, S 15.3 (CAMEBAX microprobe device, accelerating voltage 15 kV, collection time 100 s) which is also in agreement with suggested composition $Ni_9Sn_2S_2$ (at. % Ni 69.2, Sn 15.4, S 15.4).

(23) Saunders, V. R.; Dovesi, R.; Roetti, C.; Causà, M.; Harrison, N. M.; Orlando, R.; Zicovich-Wilson, C. M. *CRYSTAL98 User's Manual*; University of Torino: Torino, Italy, 1998.
(24) (a) Hay, P. J.; Wadt, W. R. *J. Chem. Phys.* **1985**, *82*, 1, 270. (b) Freyria-Fava, F. Thesis, University of Turin, Turin, Italy, 1997.
(25) Gatti, C. *TOPOND 98 User's Manual*; CNR-CSRSRC: Milano, Italy, 1999.
(26) Laaksonen, L. *gOpenMol v.1.4*, 2001; http://www.csc.fi/~laaksone/gopenmol/gIntro.html.
(27) Lyubimtsev, A. L.; Baranov, A. I.; Fischer, A.; Kloo, L.; Popovkin, B. A. *J. Alloys Compd.*, **2002**, *340*, 167.
(28) The scheme of phase relations established is available in Supporting Information.
(29) Fleet, M. E. *Acta Crystallogr., Sect. C* **1987**, *43*, 255.

Table 3. Interatomic Distances in Ni_6SnS_2 and $Ni_9Sn_2S_2$ Crystal Structures

	Ni_6SnS_2	$Ni_9Sn_2S_2$
Ni−Ni	2.5809(4)−2.6508(7)	2.581(1)−2.6734(5)
Ni−Sn	2.5809(4)−2.6508(7)	2.5964(4)−2.6395(3)
Ni−S	2.054(4)−2.631(1)	2.045(2)−2.6448(7)

The crystal structure of $Ni_9Sn_2S_2$ is similar to that of Ni_6SnS_2, and the main difference is the presence of a double-stacked, nickel−tin block of composition $^2_\infty[Ni_8Sn_2]$ instead of $^2_\infty[Ni_5Sn]$ (Figure 1). A search for additional superstructure reflexes was performed for the Ni_6SnS_2 single crystal by examining the frames with the collection time up to 5 min, but no supercell was found.

The bonding distances for the suggested structural models are listed in Table 3. Distances between metal atoms are comparable with those in $Ni_3Sn_2S_2$[14] (Ni−Sn, 2.70−2.73 Å) and metallic Ni[30] (Ni−Ni, 2.49 Å). The shortest Ni−S bonds in the title compounds (<2.1 Å, parallel to the *c* axis, Figure 1) are shorter than the typical distance for known Ni−S bonds, which are about 2.2−2.4 Å (in NiS[31] or Ni_3S_2[32]), and the shortest Ni−S distance known in binary sulfides is 2.184 Å in Ni_9S_8.[29] A similar situation appears in $Ni_{5.72}SbSe_2$, in which rather short Ni−Se distances (2.250 Å) parallel to the *c* axis exist. Possibly, this can be attributed to the distortion of the nickel−sulfide blocks, which are forced into lattice dimensions coinciding with that of the nickel−tin block. The Sn−Sn and S−S distances in Ni_6SnS_2 and $Ni_9Sn_2S_2$ are longer than 3.6 Å, and they should be considered nonbonding.

Quantum-Chemical Calculations. The presence of partially occupied Ni sites in both structures requires ordered models to be formulated for adequate band structure calculations. Three simple models of ordering were considered for both compounds: (a) only Li_2O-type $^2_\infty[Ni_{0.5}S]$ slabs alternating with nickel−tin slabs ($^2_\infty[Ni_5Sn]$ for Ni_6SnS_2 or $^2_\infty[Ni_8Sn_2]$ for $Ni_9Sn_2S_2$), (b) same as that listed as (a), but with only NaCl-type $^2_\infty[Ni_{0.5}S]$ slabs, and (c) both NaCl- and Li_2O-type $^2_\infty[Ni_{0.5}S]$ slabs alternating regularly with $^2_\infty[Ni_5Sn]$ (Ni_6SnS_2) or $^2_\infty[Ni_8Sn_2]$ ($Ni_9Sn_2S_2$) slabs. In this model, each heterometallic slab has two neighbor sulfide slabs, one of the NaCl-type and one of the Li_2O-type.

The cell dimensions of the model unit cells were the same as those from the X-ray crystallographic examination. The partial occupation of Ni sites within each type of sulfide slab was simulated by removal of half of the Ni atoms from each type of the Ni−S slabs while the values of *a* and *b* parameters of the modeled unit cell were maintained. The mirror plane orthogonal to the *c* axis was maintained for the (a) and (b) models in order to accelerate the calculations. All three models are illustrated on Figure 2. The compositions of every model were Ni_6SnS_2 or $Ni_9Sn_2S_2$ correspondingly.

The calculated total DFT energies per unit cell for each structural model were very close (maximum difference was 0.04 au), thus also providing a rational background for the observed disorder of the sulfide slabs along the *c* axis. The calculational results for both compounds show that any model of the site ordering may be used for the theoretical studies. Therefore, model (c) of Ni_6SnS_2 is employed (see below) as a representative example, unless otherwise stated.

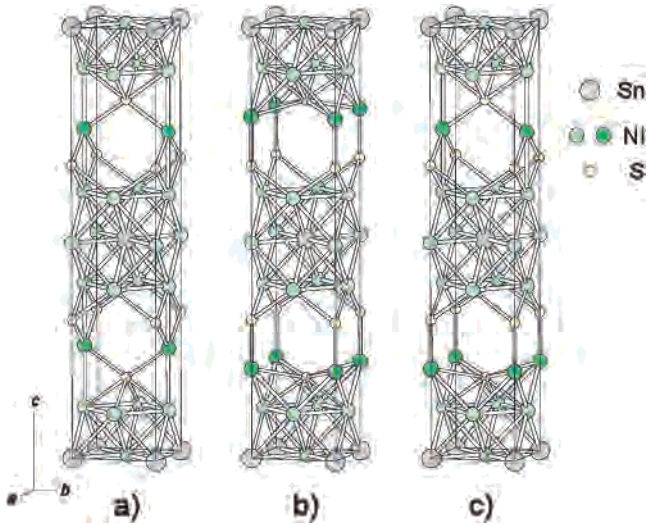

Figure 2. Unit cells of model Ni_6SnS_2 crystal structures employed in calculations.

The calculated band structure and density of states (DOS) for Ni_6SnS_2 are shown in Figure 3. No pronounced anisotropy of the band structure can be observed from Figure 3a. Total and projected DOS curves (Figure 3b) show that the Ni states are almost fully occupied and the DOS at the Fermi level is low but not zero. This suggests metallic conductivity and Pauli paramagnetic behavior of Ni_6SnS_2. The states of the Ni atoms inside the heterometallic slabs [those denoted Ni(a) in Figure 3b are equal to Ni(1) and Ni(2) in Ni_6SnS_2] and those of the Ni atoms inside sulfide slabs [those denoted Ni(b) in Figure 3b are equal to Ni(3) and Ni(4) in Ni_6SnS_2] reside in nearly the same energy range, although their coordination is quite different.

The calculated Mulliken charges for Ni_6SnS_2 are positive for Sn (+0.8) and negative for S (−1.2). The charge of the Ni atoms varies from close to zero for Ni(1) (in the center of heterometallic slabs) via +0.2 for Ni(2) (on the Ni−Sn block boundary) to +1 for Ni(3) and Ni(4) (inside the sulfide slab).

The difference charge density map inside the heterometallic slabs is shown in Figure 4a. Isosurfaces marked A correspond to 4-center bonding interactions between nickel and tin (3Ni + Sn).

The interactions inside the rock salt sulfide slabs are classical pairwise Ni−S interactions, as can be seen by the B isosurfaces on the appropriate Ni−S contact vectors (Figure 4b). At the same time, the bonding between the nickel−sulfide and the heterometallic slabs is of multicenter nature (2Ni + S), as shown by the C maxima (Figure 4b). Both pairwise Ni−S (D and E) and 3-center (2Ni + S) interactions (F) also exist in the antifluorite slabs (Figure 5).

The general conclusions drawn from the calculation results for $Ni_9Sn_2S_2$ are the same as those for Ni_6SnS_2. One of the

(30) Swanson, H. E.; Tatge, E. U.S. National Bureau of Standards, Circ. 539, I, 13, 1953.
(31) Rajamani, V.; Prewitt, C. T. *Can. Mineral.* **1974**, *12*, 253.
(32) Parise, J. B. *Acta Crystallogr., Sect. B* **1980**, *36*, 1179.

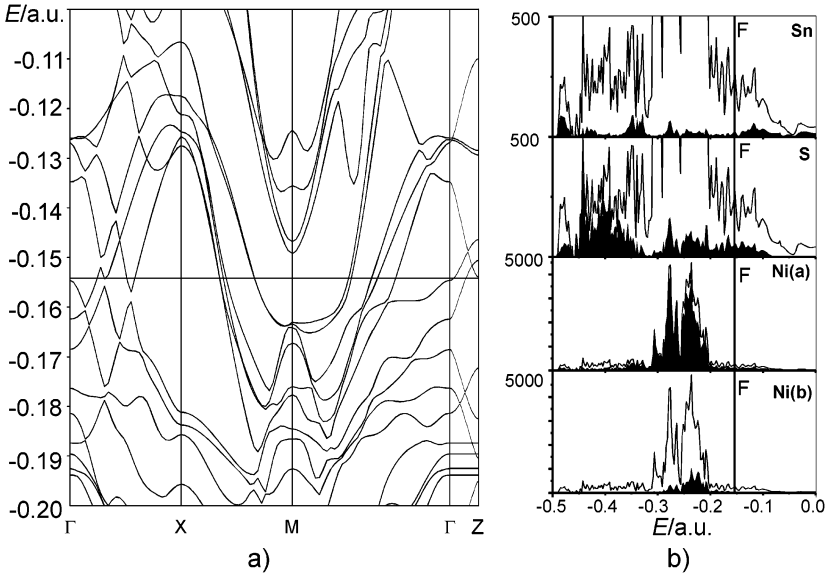

Figure 3. Electronic structure for Ni_6SnS_2 with both types of sulfide slabs (model c). Ni(a) stands for nickel atoms inside heterometallic slabs; Ni(b) stands for nickel atoms inside sulfide slabs.

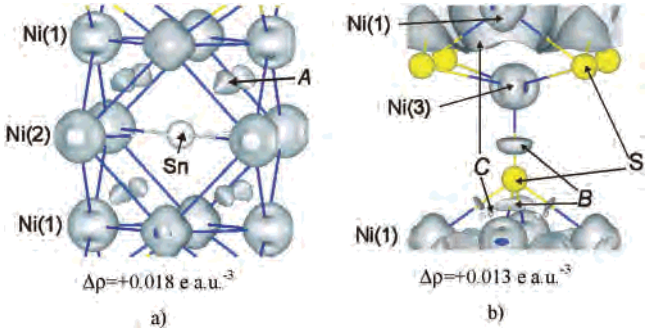

Figure 4. Difference charge density inside the heterometallic slab (a) and sulfide slab of NaCl-type (b) in Ni_6SnS_2. The latter map was calculated for Ni_6SnS_2 containing only rock-salt-type slabs.

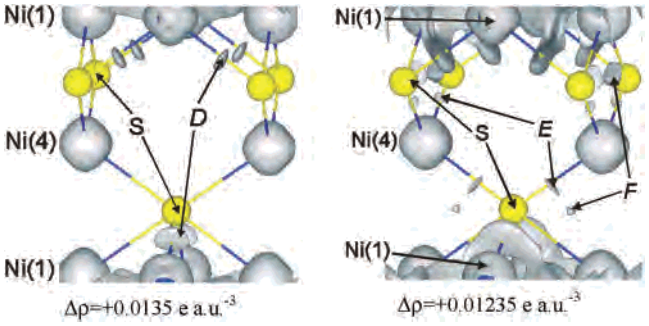

Figure 5. Difference charge density inside the sulfide slabs of antifluorite-type for Ni_6SnS_2.

most noticeable difference concerns the Mulliken charge values. For example, the Ni atoms in the center of the double heterometallic blocks carry somewhat more negative charge (ca. −0.2) as compared with Ni_6SnS_2, which is likely because of the difference in the stoichiometry.

Discussion

As already mentioned, both title compounds can be viewed as composed of heterometallic and sulfide 2D slabs alternating along the crystallographic *c* axis. The infinite system of metal−metal bonds is restricted by sulfur atoms to two dimensions in such a way that the heterometallic slabs are isolated from each other by the nonmetal atoms. Moreover, the performed quantum-chemical calculations revealed the bonding within the bimetallic slabs to have a delocalized multicenter nature, which is characteristic for metallic systems,[27,33] while mostly classical pairwise bonding exists between nickel and sulfur. Consequently, two different types of chemical bonds exist in such compounds, which therefore, from the viewpoint of the nature of the chemical bond, can be regarded as "layered".

From a synthetic point of view, it is interesting to note the dimensionality effects of adding nonmetal components going from binary to ternary or quarternary systems. Although being structurally anisotropic, the binary compound Ni_3Sn can be regarded as a 3D metal.[27] The two ternary compounds of this work, invoking sulfur in addition to the metals, isolate 2D metallic structural entities between rock-salt-like Ni−S slabs, thus confining the metal−metal bond system to two dimensions. Although containing a different main-group component, Bi instead of Sn, the recently investigated Ni_8Bi_8SI compound contains ternary columns of 1D heterometallic bonds separated by the iodine in the form of iodide ions, electronically isolating the columns.[15] This trend may be a useful general guideline in the systematic search for low-dimensional electronic properties.

So far, only a few mixed metal-rich chalcogenides with alteration of metal and nonmetal 2D blocks have been reported. To our knowledge, only the mixed nickel−antimony chalcogenides $Ni_{5.72}SbSe_2$ and $Ni_{5.66}SbTe_2$,[10] and the mixed tellurides of scandium and group 10−12 metals Sc_6MTe_2 (M = Pd;[34] M = Cu, Ag, Cd[8]), exist in the literature.

The crystal structures of the nickel−antimony chalcogenides $Ni_{7-x}SbQ_2$ (Q=Se, Te) are related to the structures reported in this work and can be viewed as composed of

(33) Silvi, B.; Gatti, C. *J. Phys. Chem. A* **2000**, *104*, 947.
(34) Maggard, P. A.; Corbett, J. D. *J. Am. Chem. Soc.* **2002**, *122*, 10740.

heterometallic and nickel−chalcogenide slabs stacked along the crystallographic *c* axis, namely $^2_\infty[Ni_5Sb]$ and $^2_\infty[Ni_yQ_2]$ ($y = 0.72$ for Q = Se, and $y = 0.66$ for Q = Te) with the atoms arranged in Cu_3Au and rock salt motifs, respectively. These are related to the $^2_\infty[Ni_5Sn]$ and $^2_\infty[Ni_{0.5}S]$ slabs in Ni_6SnS_2 and $Ni_9Sn_2S_2$, although the nickel−chalcogenide slab of the antifuorite-type is absent in the structures of the nickel−antimony chalcogenides. The occupancy factor for the Ni site within the rock-salt-type slab is about $^1/_3$ in $Ni_{7-x}SbCh_2$ and close to $^1/_2$ in Ni_6SnS_2 and $Ni_9Sn_2S_2$. Partially occupied Ni sites are common in the crystal structures of nickel chalcogenides such as β-Ni_3S_2.[35]

In the mixed scandium tellurides Sc_6MTe_2 (M = Pd, Ag, Cu, Cd), the metal atoms are arranged in an entirely different structural motif forming puckered 2D heterometallic slabs joined by tellurium atoms. The late d-metal site in the copper-containing compound is occupied by Cu and Te atoms simultaneously (occupancies of 0.8 for Cu and 0.2 for Te; real composition $Sc_6Cu_{0.8}Te_{2.2}$).

The title compounds represent an interesting example of phases with infinite, two-dimensional metal slabs tied together by nonmetal atoms. The new feature is that not only single-stacked but also double-stacked heterometallic slabs are obtained. No other new ternary nickel−tin sulfides were found in our investigation, and hence, no triple, quadruple, or more extended bimetallic slabs are obtained under the specified conditions of synthesis. Possibly, this can be explained by the higher stability of a hexagonal structure for the ultimate slab composition Ni_3Sn, rather than the cubic structure of the Cu_3Au-type. Another interesting feature of the compounds in question is the presence of sulfide slabs of defect Li_2O- and NaCl-types, while in the mixed antimony chalcogenides only the latter appears. Probably, this could be attributed to the lower stability of the antifluorite-type structure, where the coordination number of nickel is four. Such a small coordination number in the presence of big Se and Te makes a defect rock-salt-type slab with a higher coordination number of nickel energetically more favorable.

As already mentioned, the quantum-chemical calculations show that the nature of the chemical bond is quite different inside the heterometallic and sulfide slabs. Multicenter bonds between nickel and tin appear to be the most pronounced bonds in these compounds; pairwise Ni−S bonds are also significant as deduced from the $\Delta\rho$ values. No calculations were performed for the $Ni_{7-x}SbCh_2$ phases, but EHT-level calculations have been made for the mixed scandium tellurides.[8] Although the COOP analysis employed only invokes pairwise interactions, it also showed intermetallic Sc−Sc, Sc−Ag, and Sc−Te interactions to be the predominant ones. The calculated Mulliken charges of metal atoms increase from the interior of the heterometallic slab to its exterior in the mixed scandium tellurides, just as for the compounds in the present work. Consequently, a concentration of charge inside the heterometallic slabs bounded by sulfur atoms can be a general feature of this type of compounds, indicating a tendency by sulfur atoms to withdraw the electrons from the metal. It is reasonable to regard the heterometallic slab as "a piece of metal" that can act as a virtual "electronic reservoir"; the intermetallic bonds are nonsaturated with respect to the number of electrons.[33] Consequently, element substition ought to be feasible in such compounds. EHT calculations performed also verify the potential electronic capacity of mixed scandium tellurides.[8]

The infinite metallic system observed in the Ni−Sn−S compounds suggest 2D metallic conductivity. Nethertheless, no significant anisotropy of conductivity is evident from the calculated band structure of nickel−tin sulfides, although the infinite structural metallic system is only two-dimensional. Unfortunately, no information on anisotropic physical properties, neither experimental or theoretical, is available. Therefore, it is not clear if the two-dimensional nature of the bimetallic slabs is manifested in anisotropic physical properties.

Acknowledgment. The authors thank Prof. A. V. Shevelkov for the discussion of the results. This work was supported by program "Universities of Russia" (UR-05.03.011) and the INTAS program (Grant 99-1672).

Supporting Information Available: Phase relation scheme in the ternary Ni−Sn−S system at 540 °C. X-ray crystallographic file for Ni_6SnS_2 and $Ni_9Sn_2S_2$ (CIF). Basis set and input coordinates used in the calculations of electronic structures with the CRYSTAL98 software. The material is available free of charge via the Internet at http://pubs.acs.org.

IC034349+

(35) Line, G.; Huber, M. *C. R. Hebd. Seances Acad. Sci.* **1963**, *256*, 3118.